Miscoding Events during DNA Synthesis Past the Nitration-Damaged Base 8-Nitroguanine†

Naomi Suzuki,‡ Manabu Yasui,‡ Nicholas E. Geacintov,§ Vladimir Shafirovich,§ and Shinya Shibutani*,‡

Laboratory of Chemical Biology, Department of Pharmacological Sciences, State University of New York at Stony Brook, Stony Brook, New York 11794-8651, and Department of Chemistry, New York University, New York 10003

Received February 15, 2005; Revised Manuscript Received May 3, 2005

ABSTRACT: 8-Nitro-2′-deoxyguanosine (8-NO_2-dG) DNA adducts are induced by the reactive nitrogen species and may be associated with the development of cancer in inflammatory tissues. To explore the miscoding potential of 8-NO_2-dG adduct, an oligodeoxynucleotide containing a single 8-NO_2-dG adduct was prepared by photochemical synthesis and used as a template in primer extension reactions catalyzed by mammalian DNA polymerases (pol). Primer extension reactions catalyzed by pol α or *β* were strongly retarded at the 8-NO_2-dG lesion; a fraction of primers was extended past the lesion by incorporating preferentially dCMP, the correct base, opposite the lesion, accompanied by lesser amounts of dAMP and dGMP incorporation. In contrast, primer extension reactions catalyzed by pol *η* or a truncated form of pol *κ* (pol *κ*ΔC) readily extended past the 8-NO_2-dG lesion. Pol *η* and *κ*ΔC showed more broad miscoding spectra; direct incorporations of dCMP and dAMP were observed, along with lesser amounts of dGMP and dTMP incorporations and deletions. The miscoding frequencies induced by pol *η* and *κ*ΔC were at least 8 times higher than that of pol α or *β*. Miscoding frequency and specificity of 8-NO_2-dG varied depending on the DNA polymerases used. These observations were supported by steady-state kinetic studies. 8-NO_2-dG adduct may play an important role in initiating inflammation driven carcinogenesis.

Nitric oxide (•NO) is a product of normal methabolic activity in vivo and is overproduced in response to various diseases such as chronic inflammatory, reperfusion injury, and cancer (*1*, *2*). •NO generates endogenously as through the L-arginine oxidation pathway catalyzed by NADPH-dependent •NO synthase (*3*, *4*) and functions in nerve tissue, blood vessels, and immune system as a multifunctional bioregulator (*5*−*8*). •NO also is formed by the combustion of fossil fuels and cigarettes (*9*−*13*). •NO produces nitroso- (e.g., *S*-nitrosoglutathione) and nitro- (e.g., 3-nitrotyrosine) compounds in many tissues such as brain and vascular tissues (*14*−*20*) and reacts with cellular DNA to form 2′-deoxyxanthosine (dXao[1]) (*21*−*23*) and 8-nitro-2′-deoxyguanosine (8-NO_2-dG) (*24*, *25*). There are two possible major pathways for the •NO reaction (Figure 1). One pathway involves nitrosative deamination of DNA bases by •NO via formation of several nitrosating agents, which predominantly exist as

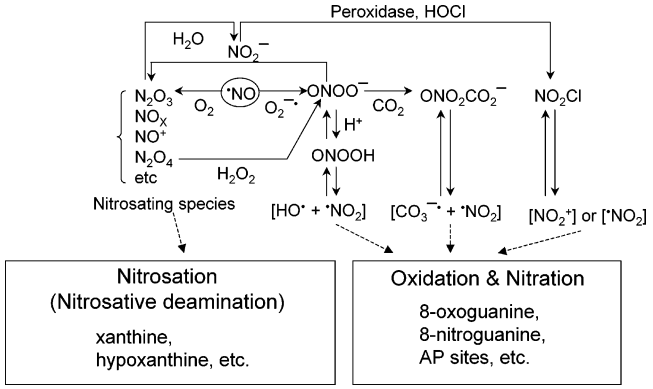

FIGURE 1: Possible pathways for formation of NO-induced DNA adducts.

nitrous anhydride (N_2O_3) at physiological pH (*26*). A second involves combination of •NO and superoxide with formation of highly toxic peroxynitrite ($ONOO^-$). Spontaneous hydrolysis of peroxynitrite under physiological conditions generates secondary radical species ($•NO_2$ and •OH) that induce nitration and oxidation of diverse biomolecules (*27*, *28*); carbonate radical anions ($CO_3^{-•}$) are also produced in the presence of CO_2. 8-NO_2-dG is formed via addition of nitrogen dioxide radical ($•NO_2$) to the C8 position of the neutral 2′-deoxyguanosine radical [dG(−H)•] derived from one-electron oxidation of guanine residues by $CO_3^{-•}$ (*29*). The addition of $•NO_2$ to the C5 position of dG(−H)• culminates in the formation of 5-guanidino-4-nitroimidazole lesion as another nitrated DNA adduct (*30*).

8-NO_2-dG adduct was detected in the peripheral lymphocyte of humans exposed to cigarette smoke (*31*) and in the

†This research was supported in part by Grants ES04068 and ES09418 (to S.S.) from the National Institute of Environmental Health Sciences, and Grant-in-aid (to M.Y.) from Japan Society for the Promotion of Science (JSPS, Japan). The portion of the work performed at New York University was supported by NIH grant ES11589.

* To whom correspondence should be addressed. Phone: 631-444-8018. Fax: 631-444-3218. E-mail: shinya@pharm.sunysb.edu.

‡ SUNY at Stony Brook.

§ New York University.

[1] Abbreviations: 8-NO_2-dG, 8-nitro-2′-deoxyguanosine; 8-NO_2-G, 8-nitro-2′-guanine; dXao, 2′-deoxyxanthosine; 8-oxodG, 7,8-dihydro-8-oxodeoxyguanosine; dNTP, 2′-deoxynucleoside triphosphate; pol α, DNA polymerase α; pol *β*, DNA polymerase *β*; pol *η*, DNA polymerase *η*; pol *κ*, DNA polymerase *κ*; pol *κ*ΔC, a truncated form of pol *κ*; F_{ins}, frequency of insertion; F_{ext}, frequency of extension; PAGE, polyacrylamide gel electrophoresis.

10.1021/bi050276p CCC: $30.25
Published on Web 06/01/2005

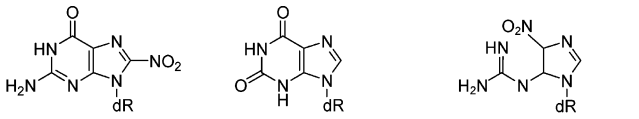

FIGURE 2: Structures of major NO-induced DNA adducts.

gastric gland epithelium of patients with *Helicobacter pylori* infection (*32*). The increased formation of 8-NO_2-dG was also observed in the *Opisthorchis viverrini*-infected hamsters used as a model animal of chronic inflammation (*33*) and in mice with inflammatory bowel disease (*34*). 8-NO_2-dG is spontaneously hydrolyzed under physiological conditions, resulting in release of free base 8-NO_2-G and formation of apurinic sites in DNA (*25*). Since the resultant apurinic sites induce G → T transversions (*35*, *36*), the mutagenicity of 8-NO_2-dG is thought to result from the miscoding event associated with the depurination of this adduct.

Many DNA polymerases are involved in DNA synthetic events in cells, and the physiological significance of these enzymes has been reviewed (*37*). Among them, human DNA pol η (*38*) and κ (*39*, *40*) are associated with translesion synthesis past a variety of DNA lesions (*41*, *42*). We present here a quantitative determination of the miscoding frequencies and specificity of 8-NO_2-dG lesion occurring during in vitro DNA replication catalyzed by mammalian DNA polymerases using a two-phase polyacrylamide gel electrophoresis analysis that quantifies base substitutions and deletions (*43*, *44*). Relative bypass frequencies past the 8-NO_2-dG lesion were also determined using steady-state kinetic studies (*45*, *46*).

MATERIALS AND METHODS

General. [γ-^{32}P]ATP (specific activity > 6000 Ci/mmol) was obtained from Amersham Corp. dNTPs were from Pharmacia; T4 polynucleotide kinase was from Stratagene. *Eco*RI restriction endonuclease (100 units/μL) and T4 DNA ligase (400 units/μL) were purchased from New England BioLabs. HPLC-grade acetonitrile, triethylamine, and distilled water were purchased from Fisher Chemical.

Synthesis of Oligodeoxynucleotides. Unmodified DNA templates (5′CCTTCGCTACTTTCCTCTCCATTT and 5′CATGCTGATGAATTCCTTCGCTACTTTCCTCTCCATTT), primers, and standard markers (Figure 2) were prepared by solid-state synthesis on an automated DNA synthesizer. The 24-mer oligodeoxynucleotide containing a single 8-NO_2-dG located at the X position (5′CCTTCXCTACTTTCCTCTCCATTT, where X is 8-NO_2-dG) was prepared by photochemical synthesis described early (*29*). Modified 38-mer templates (5′CATGCTGATGAATTCCTTCXCTACTTTCCTCTCCATTT, where X is 8-NO_2-dG) were prepared by ligation of the 8-NO_2-dG-modified 24-mer to a 14-mer (5′CATGCTGATGAATT) (*47*). Briefly, 2.0 μg of 8-NO_2-dG-modified 24-mer was phosphorylated at the 5′ terminus using 3.0 μL of T4 polynucleotide kinase (10 units/μL) and 1.5 μL of 10 mM ATP and ligated at 4 °C overnight to a 14-mer (1.75 μg, 5′CATGCTGATGAATT) using 1.5 μL of T4 DNA ligase (400 units/μL) and a 18-mer template (2.25 μg, 5′GTAGCGAAGGAATTCATC) in 100 μL of 50 mM Tris-HCl (pH 7.5) containing 10 mM $MgCl_2$, 10 mM DTT, 1 mM ATP, and 2.5 μg of BSA. The 38-mer product was isolated on a μBondapak C_{18} column (0.39 cm × 30 cm), using a linear gradient of 0.05 M triethylammonium acetate (pH 7.0) containing 10−20% acetonitrile, with an elution time of 60 min at a flow rate of 1.0 mL/min. The modified and unmodified oligomers were purified using HPLC and gel electrophoresis. Oligodeoxynucleotides were labeled at the 5′ terminus with ^{32}P (*48*) and subjected to 20% polyacrylamide gel electrophoresis (PAGE, 35 cm × 42 cm × 0.04 cm). The positions of the bands and homogeneities of oligodeoxynucleotides following gel electrophoresis were determined using a β-phosphorimager (Molecular Dynamics). Separation and purification of oligodeoxynucleotides was performed using a Waters 515 HPLC pump, 996 photodiode array detector and pump control module. UV spectra and concentrations of oligodeoxynucleotides were measured with a Hewlett-Packard 8452A diode array spectrophotometer.

Stability of 8-NO_2-dG-Modified Oligomer. ^{32}P-labeled 8-NO_2-dG-modified and -unmodified oligomers (10 pmol, 5′CCTTCXCTACTTTCCTCTCCATTT, where X is dG or 8-NO_2-dG) were prepared by incubating at 25 °C for 15 min using T4 polynucleotide kinase and [γ-^{32}P]ATP (*48*) and passed through a molecular filter to remove free ^{32}P and buffer. The ^{32}P-labled oligomers were incubated at 25 °C in 50 μL of buffer (40 mM Tris-HCl (pH 8.0), 1 mM $MgCl_2$, 10 mM DTT, 250 μg/mL BSA, 60 mM KCl, and 2.5% glycerol), which was used for primer extension reactions catalyzed by pol η. To measure the degradation rate of the 8-NO_2-dG-modified oligomers, an aliquot (2 μL) of the reaction mixture was collected at 0, 0.5, 2, and 6 h and subjected to 20% denaturing PAGE (35 cm × 42 cm × 0.04 cm). The radioactivity of the oligomers was measured using β-phosphorimager (Molecular Dynamics) and ImageQuaNT software.

Primer Extension Reactions. A 10-mer (5′AGAGGAAAGT) or 12-mer (5′AGAGGAAAGTAG) was labeled at the 5′ terminus with T4 polynucleotide kinase and [γ-^{32}P]ATP (*48*). Using 8-NO_2-dG-modified and -unmodified 38-mer oligodeoxynucleotide (200 fmol) primed with a ^{32}P-labeled 10-mer (100 fmol) or 12-mer (100 fmol), we conducted primer extension reactions catalyzed by pol α, β, η, or κ at 25 °C for 30 min in a buffer (10 μL) containing four dNTPs (100 μM each) (Figure 3). The reaction buffer for pol α contains 40 mM Tris-HCl (pH 8.0), 5 mM $MgCl_2$, 60 mM KCl, 10 mM dithiothreitol (DTT), 250 μg/mL BSA, and 2.5% glycerol. The reaction buffer for pol β contains 50 mM Tris-HCl (pH 8.8), 10 mM $MgCl_2$, 10 mM KCl, 1.0 mM DTT, and 1.0% glycerol. Pol η and a truncated form (pol $\kappa\Delta$C) and full-length of pol κ were provided by Dr. Hanaoka and Dr. Ohmori, respectively. (*38*, *39*). The reaction buffer for pol η contains 40 mM Tris-HCl (pH 8.0), 1 mM $MgCl_2$, 10 mM DTT, 250 μg/mL BSA, 60 mM KCl, and 2.5% glycerol. A similar reaction buffer was used for pol $\kappa\Delta$C, using 5 mM $MgCl_2$ instead of 1 mM $MgCl_2$. The reaction was stopped by addition of formamide dye. The samples were subjected to 20% denaturing PAGE (35 cm × 42 cm × 0.04 cm). The radioactivity of extended products was measured using a β-phosphorimager and ImageQuaNT software.

Miscoding Analysis. Using 8-NO_2-dG-modified and -unmodified 38-mer oligodeoxynucleotide (450 fmol) primed with a ^{32}P-labeled 12-mer (300 fmol,5′AGAGGAAAGTAG), we conducted primer extension reactions catalyzed by pol

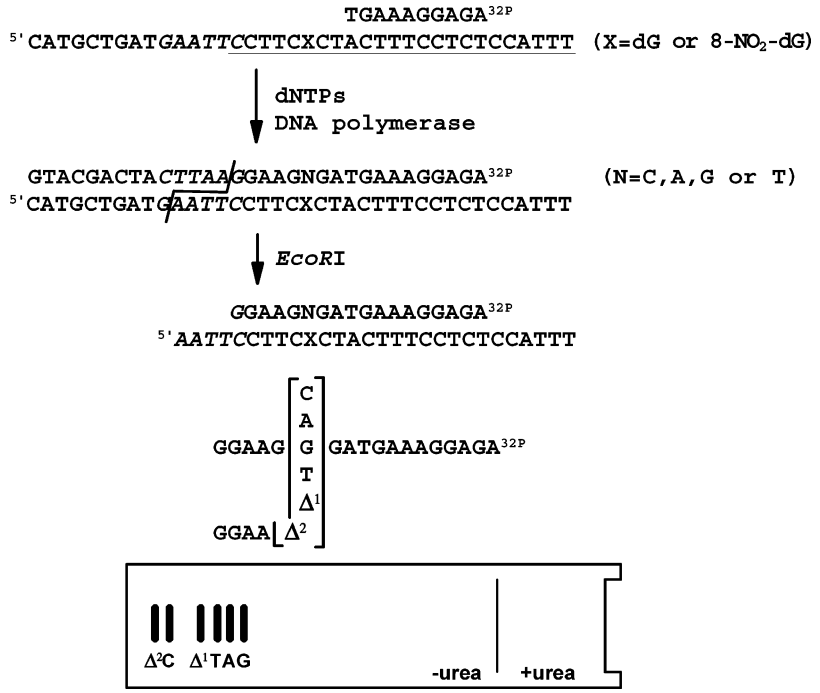

FIGURE 3: Diagram of the method used to determine miscoding specificity. Unmodified and 8-NO_2-dG-modified 38-mer templates are annealed to either a ^{32}P-labeled 10-mer primer or a ^{32}P-labeled 12-mer primer. Primer extension reactions catalyzed by DNA pol α, *β*, *η*, or *κ* were conducted in the presence of four dNTPs. Fully extended products formed during DNA synthesis were recovered from the polyacrylamide gel (35 cm × 42 cm × 0.04 cm), annealed with a complementary 38-mer, cleaved with *Eco*RI, and subjected to a two-phase PAGE (15 cm × 72 cm × 0.04 cm), as described in Materials and Methods. To determine miscoding specificity, mobilities of the reaction products were compared with those of the 18-mer standards containing dC, dA, dG, or dT opposite the lesion and one- (Δ^1) or two-base (Δ^2) deletions.

α (80 fmol for unmodified template; 250 fmol for 8-NO_2-dG-modified template), pol *β* (250 fmol for unmodified template; 500 fmol for 8-NO_2-dG-modified template), pol *η*, or pol *κ*ΔC (100 fmol for the unmodified and modified templates) at 25 °C for 30 min in a buffer (30 *μ*L) containing four dNTPs (100 *μ*M each) and subjected to 20% PAGE (35 cm × 42 cm × 0.04 cm). Extended reaction products (>26 bases long) were extracted from the gel. The recovered oligodeoxynucleotides were annealed with an unmodified 38-mer, cleaved with *Eco*RI, and subjected to two-phase PAGE (15 cm × 72 cm × 0.04 cm) containing 7 M urea in the upper phase and no urea in the lower phase (*44*) (Figure 3). To quantify base substitutions and deletions, mobilities of the reaction products are compared with those of 18-mer standards containing dC, dA, dG, or dT opposite the lesion and one- (Δ^1) or two-base (Δ^2) deletions (*43*, *44*) (Figure 3).

Steady-State Kinetic Studies. Kinetic parameters associated with nucleotide insertion opposite 8-NO_2-dG lesion and chain extension from the 3′ primer terminus were determined at 25 °C using varying amounts of single dNTPs (0−500 *μ*M). For insertion kinetics, reaction mixtures containing dNTP (0−500 *μ*M) and either pol α (25−250 fmol), pol *β* (30−300 fmol), pol *η* (0.16−1.6 fmol), or pol *κ*ΔC (0.29−2.9 fmol) were incubated at 25 °C for 2 min in 10 *μ*L of Tris-HCl buffer (pH 8.0) using a 24-mer template (150 fmol; 5′CCTTCXCTACTTTCCTCTCCATTT, where X is dG or 8-NO_2-dG) primed with a ^{32}P-labeled 12-mer (100 fmol; 5′AGAGGAAAGTAG). Reaction mixtures containing a 24-mer template (150 fmol) primed with a ^{32}P-labeled 13-mer (100 fmol; 5′AGAGGAAAGTAGN, where N is C, A, G, or T), with varying amounts of dGTP (0−500 *μ*M) and either pol α (25−250 fmol), pol *β* (30−300 fmol), pol *η* (0.16−1.6 fmol), or pol *κ*ΔC (0.29−2.9 fmol) were used to measure chain extension. The reaction samples were subjected to 20% denaturing PAGE (35 cm × 42 cm × 0.04 cm). The Michaelis constants (K_m) and maximum rates of reaction (V_{max}) were obtained from Hanes−Woolf plots. Frequencies of dNTP insertion (F_{ins}) and chain extension (F_{ext}) were determined relative to the dC/dG base pair according to the equation $F = (V_{max}/K_m)_{[\text{wrong pair}]}/(V_{max}/K_m)_{[\text{correct pair=dC/dG}]}$ (*45*, *46*).

RESULTS

Primer Extension Reactions Catalyzed by DNA Polymerases on the 8-NO_2-dG-Modified DNA Template. Using unmodified and 8-NO_2-dG-modified 38-mer templates, primer extension reactions were conducted in the presence of four dNTPs and variable amounts of pol α, *β*, *η*, or *κ*ΔC (Figure 4). Primer extension with these polymerases readily occurred on the unmodified template to form fully extended products. More than 95% of the starting primer was extended past the unmodified dG (position 13) using 250 fmol of pol α (Figure 4A) or pol *β* (data not shown) and 10 fmol of pol *η* (Figure 4B) or *κ*ΔC (Figure 4C). When the 8-NO_2-dG-modified template was used, primer extension reactions catalyzed by pol α (Figure 4A) or *β* (data not shown) were retarded one base prior to the lesion and opposite the lesion. However, primer extension reactions catalyzed by pol *η* or *κ*ΔC were slightly blocked at the 8-NO_2-dG site but extended past the lesion to form the fully extended products (Figure 4B,C). When the amounts of polymerases were increased, products representing more than 32-mer bases long were produced on the unmodified and 8-NO_2-dG-modified templates. These are blunt-end extension products, as reported earlier for *Escherichia coli* and mammalian DNA polymerases (*49*, *50*).

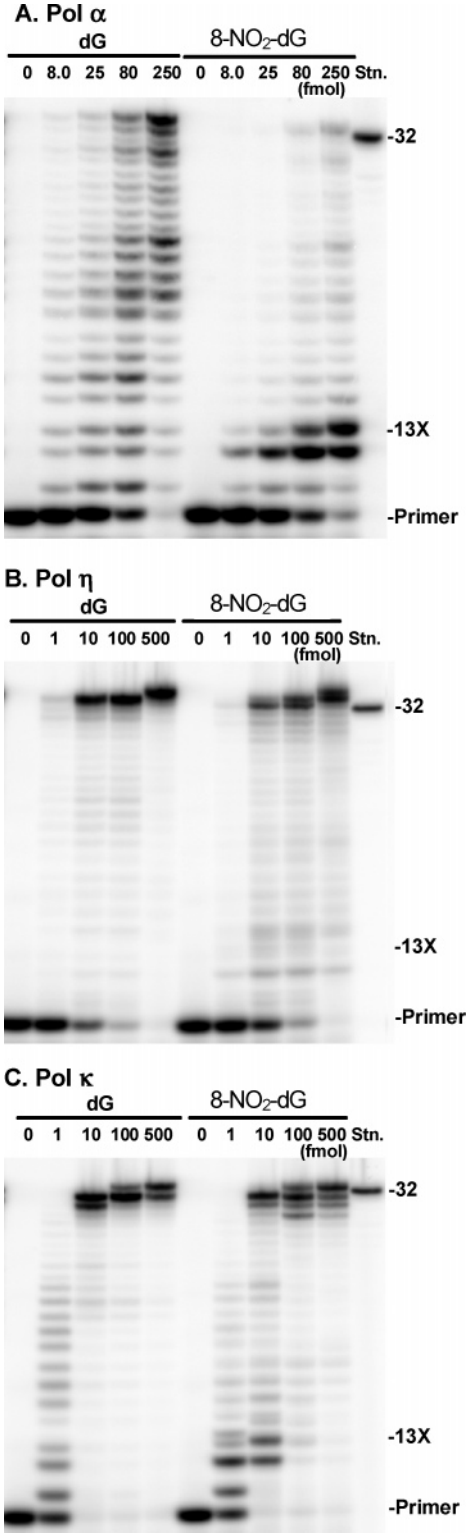

FIGURE 4: Primer extension reactions catalyzed by pol α, *η*, or *κ*ΔC on 8-NO_2-dG-modified DNA templates. Using unmodified or 8-NO_2-dG-modified 38-mer templates primed with a ^{32}P-labeled 10-mer, we performed primer extension reactions at 25 °C for 30 min in a buffer containing four dNTPs (100 *μ*M each) and variable amounts of (A) pol α (0, 8.0, 25, 80, 250 fmol), (B) pol *η* (0, 1.0, 10, 100, 500 fmol), and (C) pol *κ*ΔC (0, 1.0, 10, 100, 500 fmol), as described in Materials and Methods. One-third of the reaction mixture was subjected to denaturing 20% PAGE (35 cm × 42 cm × 0.04 cm). A 32-mer (5′AGAGGAAAGTAGCGAAGGAATTCATCAGCATG) was used as a marker of fully extended product. 13X represents the adducted position.

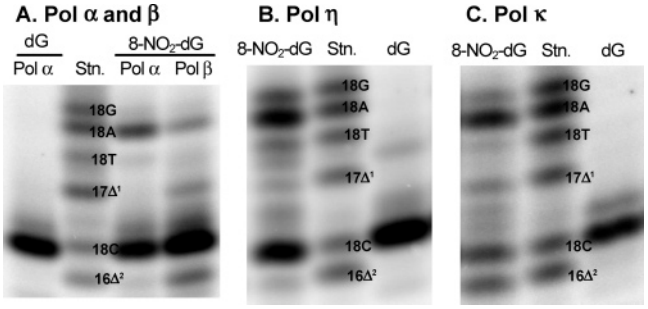

FIGURE 5: Miscoding specificities of 8-NO_2-dG lesion in reactions catalyzed by pol α, *β*, *η*, or *κ*ΔC. Using unmodified and 8-NO_2-dG-modified 38-mer templates primed with a ^{32}P-labeled 12-mer, we conducted primer extension reactions at 25 °C for 30 min in a buffer containing four dNTPs (100 *μ*M each) and either pol α (80 fmol for unmodified template; 250 fmol for 8-NO_2-dG-modified template), pol *β* (250 fmol for unmodified template; 500 fmol for 8-NO_2-dG-modified template), pol *κ*ΔC, or *η* (100 fmol for unmodified and 8-NO_2-dG-modified templates), as described in Materials and Methods. The extended reaction products (>26 bases long) produced on the unmodified and 8-NO_2-dG-modified templates was extracted following PAGE. The recovered oligodeoxynucleotides were annealed to an unmodified 38-mer and cleaved with *Eco*RI restriction enzyme, as described in Materials and Methods. A half of the reaction product from the unmodified template and the entire product from the 8-NO_2-dG-modified template were subjected to a two-phase 20% PAGE (15 cm × 72 cm × 0.04 cm). Mobilities of reaction products were compared with those of 18-mer standards **(**Figure 3) containing dC, dA, dG, or dT opposite the lesion and one-base (Δ^1) or two-base (Δ^2) deletions.

Miscoding Properties of 8-NO_2-dG Adduct. Translesion synthesis catalyzed by pol α, *β*, *η*, or *κ*ΔC was conducted in the presence of all four dNTPs. Following primer extension past 8-NO_2-dG, extended products (>26 bases long) were recovered from the gel and digested by *Eco*RI as described in Materials and Methods. Products were subjected to two-phase PAGE to quantify base substitutions and deletions formed opposite the lesion (Figure 2). A standard mixture of six ^{32}P-labeled oligodeoxynucleotides containing dC, dA, dG, or dT opposite the lesion or one- and two-base deletions can be resolved by this method (Figure 5). The percentage of miscoding was normalized to the amount of starting ^{32}P-labeled primer. When an unmodified template was used, expected incorporation of dCMP, the correct base, was observed opposite dG (Figure 5). Using pol α or *β*, 8-NO_2-dG-promoted preferential incorporation of dCMP (4.2 and 20.0%, respectively) opposite the lesion, accompanied by lesser amounts of dAMP (1.4 and 1.1%, respectively) and dTMP (0.13 and 0.38%, respectively). With pol *β*, small amounts of one- (1.4%) and two-base (2.2%) deletions were also observed. Pol *η* and *κ*ΔC showed broad miscoding specificity and high miscoding frequency. Pol *η* promoted direct incorporation of dCMP (29.7%), the correct base, and dAMP (24.5%), along with lesser amounts of dGMP (11.3%) and dTMP (7.5%) incorporations (Figure 5B); small amounts of one-base (3.9%) and two-base (2.5%) deletions were also observed. With pol *κ*ΔC, 8-NO_2-dG promoted preferential incorporation of dAMP (18.8%) opposite the lesion, accompanied by small amounts of dCMP (12.5%), dGMP (6.2%), and dTMP (3.4%) incorporations (Figure 5C); one- (4.6%) and two-base (8.9%) deletions were also detected. Therefore, total miscoding frequencies of 8-NO_2-dG observed with pol *η* (50%) and *κ*ΔC (42%) were

Table 1: Kinetic Parameters for Nucleotide Insertion and Chain Extension Reactions Catalyzed by DNA Polymerases[a]

	dNTP ↓GATGAAAGGAGA^{32P} 5′CCTTCXCTACTTTCCTCTCCATTT			dGTP ↓NGATGAAAGGAGA^{32P} 5′CCTTCXCTACTTTCCTCTCCATTT			
N:X	K_m (M)	V_{max} (% min^{-1})	F_{ins}	K_m (M)	V_{max} (% min^{-1})	F_{ext}	$F_{ins} \times F_{ext}$
			pol α; X = dG				
C:G	1.61 ± 0.15[b]	186 ± 24.1	1.0	2.39 ± 0.12	135 ± 2.3	1.0	1.0
			pol α; X = 8-NO$_2$-dG				
C:X	20.8 ± 1.88	68.7 ± 15.9	2.85×10^{-2}	3.09 ± 0.73	10.3 ± 1.5	5.93×10^{-2}	1.69×10^{-3}
A:X	116 ± 24.2	70.3 ± 1.98	5.38×10^{-3}	68.7 ± 2.2	9.40 ± 0.22	2.44×10^{-3}	1.31×10^{-5}
G:X	140 ± 15.3	22.3 ± 0.39	1.39×10^{-3}	48.7 ± 3.3	5.17 ± 0.11	1.89×10^{-3}	2.63×10^{-6}
T:X	123 ± 2.69	17.0 ± 1.07	1.20×10^{-3}	36.7 ± 1.9	10.1 ± 0.65	4.89×10^{-3}	5.87×10^{-6}
			pol η; X = dG				
C:G	1.17 ± 0.08[b]	43.8 ± 3.5	1.0	0.54 ± 0.24	33.2 ± 1.8	1.0	1.0
			pol η; X = 8-NO$_2$-dG				
C:X	2.62 ± 0.16	13.1 ± 0.46	0.133	3.55 ± 0.13	11.4 ± 0.39	5.22×10^{-2}	6.94×10^{-3}
A:X	8.89 ± 0.53	16.6 ± 1.3	4.99×10^{-2}	1.67 ± 0.29	10.5 ± 0.31	1.02×10^{-1}	5.09×10^{-3}
G:X	22.3 ± 9.0	13.1 ± 1.1	1.57×10^{-2}	5.33 ± 0.42	9.68 ± 0.10	2.95×10^{-2}	4.63×10^{-4}
T:X	21.7 ± 0.3	8.70 ± 0.40	1.07×10^{-2}	3.09 ± 0.31	7.21 ± 0.13	3.79×10^{-2}	4.06×10^{-4}
			pol κ; X = dG				
C:G	2.70 ± 0.18[b]	32.2 ± 0.83	1.0	1.53 ± 0.06	155 ± 5.4	1.0	1.0
			pol κ; X = 8-NO$_2$-dG				
C:X	15.2 ± 0.71	1.30 ± 1.1	5.69×10^{-3}	8.14 ± 0.08	9.21 ± 0.10	1.12×10^{-2}	6.37×10^{-5}
A:X	10.6 ± 3.5	1.45 ± 0.22	1.15×10^{-2}	28.2 ± 3.54	7.13 ± 0.24	2.50×10^{-3}	2.88×10^{-5}
G:X	13.4 ± 0.66	0.36 ± 0.02	2.26×10^{-3}	52.1 ± 8.71	6.11 ± 0.37	1.16×10^{-3}	2.62×10^{-6}
T:X	38.2 ± 4.5	0.08 ± 0.01	1.78×10^{-4}	9.49 ± 0.53	3.58 ± 0.08	3.72×10^{-3}	6.62×10^{-7}

[a] Kinetics of nucleotide insertion and chain extension reactions were determined as described under Materials and Methods. Frequencies of nucleotide insertion (F_{ins}) and chain extension (F_{ext}) were estimated by the equation $F = (V_{max}/K_m)_{[wrong\ pair]}/(V_{max}/K_m)_{[correct\ pair]}$. X = 8-NO$_2$-dG lesion. [b] Data are expressed as the mean ± SD.

at least 8 times higher than that of pol α (1.5%) and β (5.1%), respectively.

To determine the stability of 8-NO$_2$-dG-modified oligomer, ^{32}P-labeled 8-NO$_2$-dG-modified 24-mer (5′CCTTCXCTAC-TTTCCTCTCCATTT, where X is 8-NO$_2$-dG) was incubated at 25 °C in which the same reaction condition was used for primer extension and miscoding analysis for pol η and then analyzed using PAGE (data not shown). The degradation rate of the 8-NO$_2$-dG-modified oligomer was approximately 1.6%/h ; a similar degradation rate was observed previously (29). On the basis of our reaction condition (25 °C and 30 min) used for miscoding and primer extension assays, only 0.8% of 8-NO$_2$-dG-modified oligomer was estimated to be degraded. Such a small degradation may not affect the miscoding analysis.

Kinetic Studies on 8-NO$_2$-dG-Modified DNA Template. Using steady-state kinetic methods with DNA pol, we measured the frequency of dNTP insertion (F_{ins}) and chain extension (F_{ext}) opposite 8-NO$_2$-dG within the linear range of the reaction. With pol α, F_{ins} for dATP was 5.3 times lower than that for dCTP, the correct base, and 3.9 and 4.5 times higher than that for dGTP and dTTP, respectively (Table 1). F_{ext} for the dA/8-NO$_2$-dG pair was 24 times lower than that for the dC/8-NO$_2$-dG pair but 1.3 and 5.0 times higher than those for dG/8-NO$_2$-dG and dT/8-NO$_2$-dG pairs, respectively. Therefore, the relative bypass frequency ($F_{ins} \times F_{ext}$) past the dA/8-NO$_2$-dG pair was 129 times lower than that for dC/8-NO$_2$-dG, and 5.0 and 2.2 times higher than for the dG/8-NO$_2$-dG and dT/8-NO$_2$-dG pairs, respectively. With pol η, F_{ins} for dATP was 2.7 times lower than that for dCTP and 3.2 and 4.7 times higher than that for dGTP and dTTP, respectively (Table 1). However, F_{ext} for the dA/8-NO$_2$-dG pair was 2.0 times higher than that for the dC/8-NO$_2$-dG pair and 3.5 and 2.7 times higher than for the dG/8-NO$_2$-dG and dT/8-NO$_2$-dG pairs, respectively. Therefore, $F_{ins} \times F_{ext}$ for the dA/8-NO$_2$-dG pair (5.09×10^{-3}) was similar to that for the dC/8-NO$_2$-dG pair (6.94×10^{-3}) but 1 order of magnitude higher than that for other pairs. When pol κΔC was used, F_{ins} for dATP was 2.0 times higher than that for dCTP (Table 1). F_{ext} for the dA/8-NO$_2$-dG pair was 6.7 times lower than that for the dC/8-NO$_2$-dG pair. As a result, $F_{ins} \times F_{ext}$ for the dA/8-NO$_2$-dG pair (2.88×10^{-5}) was slightly lower that for the dC/8-NO$_2$-dG pair (6.37×10^{-5}) but at least 1 order of magnitude higher than that for other pairs.

DISCUSSION

The 8-NO$_2$-dG lesions in DNA are unstable and depurinate by releasing 8-NO$_2$-G (*25*), suggesting that the dupurinated lesion contributes to NO-mutagenic events (*35*, *36*). The half-life of 8-NO$_2$-dG-modified oligodeoxynucleotide at 23 °C in a buffer (pH 7) was previously determined to be ~20 h, although the stability of the lesion may depend on the composition of the buffer incubated, oligomer sequence, DNA secondary structure, and so forth (*29*). In fact, the degradation rate of 8-NO$_2$-dG-modified oligomer used in the present study was 1.6%/h (the half-life = 31 h) at 25 °C. Therefore, the slow rate of degradation at 25 °C allowed us to explore the miscoding events of 8-NO$_2$-dG during trans-lesion synthesis catalyzed by mammalian DNA polymerases.

The miscoding specificity of 8-NO$_2$-dG was determined using an in vitro experimental system that can quantify base substitutions and deletions formed during replication in the presence of four dNTPs. Although primer extension reactions catalyzed by pol α and β were strongly blocked at the 8-NO$_2$-dG lesion, significant amounts of dAMP misincorporation

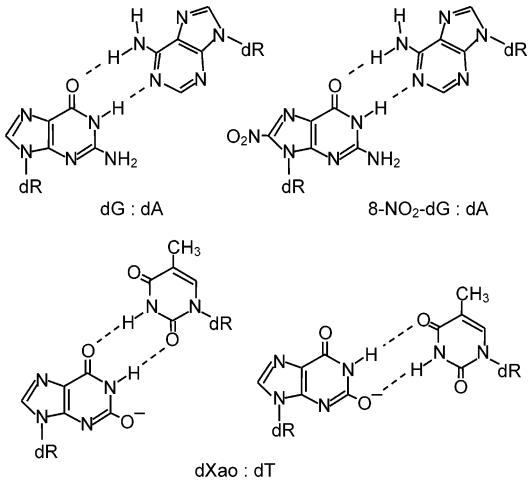

FIGURE 6: Proposed base-pairing structures involving 8-NO_2-dG.

were observed. Primer extension past the lesion with either pol η or $\kappa\Delta$C was more efficient and showed a higher miscoding frequency and broad miscoding specificity. Both pol η or $\kappa\Delta$C promoted preferential incorporation of dAMP opposite the lesion, along with the lesser amounts of dGMP and dTMP incorporation and deletions. Although the rate of primer extension reaction catalyzed by a full-length pol κ was increased approximately 10% than that of the truncated form (pol $\kappa\Delta$C), the miscoding specificities observed with both enzymes were identical (data not shown). Therefore, 8-NO_2-dG is expected to generate primarily G → T transversions in cells. Using this system, we used the fully extended products (>26 bases long) formed at 25 °C in 30 min for analysis of miscoding properties. On the basis of the degradation rate, only less than 0.8% of 8-NO_2-dG-modified template was estimated to be depurinated. The contribution of apurinic sites to the high frequency of miscoding events observed with pol η and $\kappa\Delta$C may be minimal.

Even using lower molar amounts of pol η or $\kappa\Delta$C (100 fmol), primer extension past the 8-NO_2-dG adduct was much higher than that observed with pol α (250 fmol) and β (500 fmol). As a result, the higher miscoding frequencies (50% for pol η and 42% for pol $\kappa\Delta$C) were at least 8 times greater than those for pol α (1.5%) and β (5.1%). Although all enzymes primarily promoted dAMP incorporation opposite the lesion, pol η or $\kappa\Delta$C showed broad miscoding spectra and significant amounts of dGMP and dTMP incorporation. In addition, deletions were also detected. Therefore, the miscoding frequencies and specificities vary depending on the DNA polymerase used.

When similar experimental systems were used, dXao, another major NO-induced DNA adduct, preferentially incorporated dTMP opposite the lesion, generating G → A mutations (*51*). The miscoding specificity of dXao differs from that of 8-NO_2-dG which promoted primarily G → T mutations. dXao, which exists as 6-keto-2-enolate anion in neutral solution (*52*, *53*), can pair with dT through two hydrogen bonds in a Watson−Crick manner (*54*, *55*) (Figure 6). On the basis of the structural studies for dG/dA mismatch basepair (*56*, *57*), 8-NO_2-dG may possibly pair with dA, as shown in Figure 6. The different miscoding specificities may allow us to distinguish which NO-induced lesion(s) are involved in the mutagenic events.

The two-phase PAGE analysis was performed in the presence of four dNTPs, while the kinetic parameters were determined under conditions where only a single dNTP was present. Therefore, kinetic results obtained under the dNTP noncompetitive conditions may not be directly comparable with the data obtained from the two-phase PAGE analysis. With pol α, F_{ins} for dCTP was approximately 5 times higher than that for dAMP and F_{ext} for the dC/8-NO_2-dG pair was 24 times higher than that for the dA/8-NO_2-dG pair. The resulting $F_{ins} \times F_{ext}$ value for dC/8-NO_2-dG was 129 times higher than that for dA/8-NO_2-dG (Table 1). However, when the two-phase PAGE analysis was used, the direct incorporation of dCMP opposite the 8-NO_2-dG lesion was 3 times higher than that of dAMP. Similarly, with pol $\kappa\Delta$C, although $F_{ins} \times F_{ext}$ for dA/8-NO_2-dG was 2.5 times lower than that for dC/8-NO_2-dG, the 2.9-fold higher F_{ins} for dAMP than for dCMP reflects the results obtained using the two-phase PAGE analysis. Since fully extended products used for two-phase PAGE analysis were obtained after long incubation times (30 min) with DNA polymerases lacking the 3′−5′ exonuclease activity (*36*, *43*, *44*), the F_{ins} value, not F_{ext} value, of this enzyme may reflect the frequencies of dCMP and dTMP incorporation opposite the lesion.

In the earlier reports (*58*, *59*), a shuttle vector containing the *supF* gene was exposed to peroxynitrite ($ONOO^-$) in vitro and then replicated in *E. coli* or human cells for analysis of $ONOO^-$-induced mutations. Over 90% of mutations occurred at G:C base pairs, predominantly involving G:C → T:A transversions followed by G:C → C:G transversions and G:C → A:T transitions. All of the base substitution mutations were located at G or C base, presumably reflecting miscoding errors introduced by guanine modification including 7,8-dihydro-8-oxoguanine, 8-nitroguanine, and apurinic sites (*59*). 7,8-Dihydro-8-oxodeoxyguanosine (8-oxodG) lesions (*60*, *61*) and apurinic sites (*35*, *36*) induce G → T transversions, as observed with 8-NO_2-dG in the present study. When the kinetic data of 8-oxodG (*60*, *61*) and 8-NO_2-dG are compared, DNA polymerases may bypass 8-oxodG much rapidly than 8-NO_2-dG during DNA synthesis by incorporating dAMP opposite the lesion. Since amounts of these DNA modifications produced by $ONOO^-$ have not yet been determined, it is difficult to estimate the contribution of individual DNA damage to the formation of G → T mutations.

In conclusion, 8-NO_2-dG is characterized by a high miscoding potential; the miscoding frequency and specificity varies depending on the DNA polymerase used. 8-NO_2-dG contributes, together with the depurinated site, to the NO-induced mutagenic events.

ACKNOWLEDGMENT

We are grateful to Drs. F. Hanaoka and H. Ohmori for providing human pol η and pol κ, respectively.

REFERENCES

1. Dedon, P. C., and Tannenbaum, S. R. (2004) Reactive nitrogen species in the chemical biology of inflammation, *Arch. Biochem. Biophys. 423*, 12−22.
2. Estevez, A. G., Crow, J. P., Sampson, J. B., Reiter, C., Zhuang, Y., Richardson, G. J., Tarpey, M. M., Barbeito, L., and Beckman, J. S. (1999) Induction of nitric oxide-dependent apoptosis in motor neurons by zinc-deficient superoxide dismutase, *Science 286*, 2498−2500.

3. Geller, D. A., and Billiar, T. R. (1998) Molecular biology of nitric oxide synthases, *Cancer Metastasis Rev. 17*, 7−23.
4. Stuehr, D. J. (1999) Mammalian nitric oxide synthases, *Biochim. Biophys. Acta 1411*, 217−230.
5. Palmer, R. M., Ferrige, A. G., and Moncada, S. (1987) Nitric oxide release accounts for the biological activity of endothelium-derived relaxing factor, *Nature 327*, 524−526.
6. Ignarro, L. J., Buga, G. M., Wood, K. S., Byrns, R. E., and Chaudhuri, G. (1987) Endothelium-derived relaxing factor produced and released from artery and vein is nitric oxide, *Proc. Natl. Acad. Sci. U.S.A. 84*, 9265−9269.
7. Garthwaite, J., Charles, S. L., and Chess-Williams, R. (1988) Endothelium-derived relaxing factor release on activation of NMDA receptors suggests role as intercellular messenger in the brain, *Nature 336*, 385−388.
8. Lancaster, J. R., Jr., and Hibbs, J. B., Jr. (1990) EPR demonstration of iron-nitrosyl complex formation by cytotoxic activated macrophages, *Proc. Natl. Acad. Sci. U.S.A. 87*, 1223−1227.
9. World Health Organization (1977) Oxides of Nitrogen, *WHO Environ. Health Criter. 4*.
10. World Health Organization (1997) Nitrogen Oxides, *WHO Environ. Health Criter. 188*.
11. Yoshida, K., and Kasama, K. (1987) Biotransformation of nitric oxide, *Environ. Health Perspect. 73*, 201−206.
12. Bokhoven, D., and Niessen, H. J. (1961) Amounts of oxides of nitrogen and carbon monoxide in cigarette smoke, with and without inhalation, *Nature 192*, 458−459.
13. Horton, A. D., Stokely, J. R., and Guerin, M. R. (1974) Gas chromatographic determination of nitric oxide in cigarette smoke, *Anal. Lett. 7*, 177−185.
14. Kluge, I., Gutteck-Amsler, U., Zollinger, M., and Do, K. Q. (1997) *S*-nitrosoglutathione in rat cerebellum: identification and quantification by liquid chromatography-mass spectrometry, *J. Neurochem. 69*, 2599−25607.
15. Jia, L., Bonaventura, C., Bonaventura, J., and Stamler, J. S. (1996) *S*-nitrosohaemoglobin: a dynamic activity of blood involved in vascular control, *Nature 380*, 221−226.
16. Marley, R., Feelisch, M., Holt, S., and Moore, K. P. (2000) A chemiluminescence based assay for *S*-nitrosoalbumin and other plasma Snitrosothiols, *Free Radical Res. 32*, 1−9.
17. Torreilles, F., Salman-Tabcheh, S., Guerin, M., and Torreilles, J. (1999) Neurodegenerative disorders: the role of peroxynitrite, *Brain Res. Rev. 30*, 153−163.
18. Thuraisingham, R. C., Nott, C. A., Dodd, S. M., and Yaqoob, M. M. (2000) Increased nitrotyrosine staining in kidneys from patients with diabetic nephropathy, *Kidney Int. 57*, 1968−1972.
19. Akaike, T., Nogushi, Y., Ijiri, S., Setoguchi, K., Suga, M., Zheng, Y. M., Dietzschold, B., and Maheda, H. (1996) Pathogenesis, of influenza virusinduced pneumonia: involvement of both nitric oxide and oxygen radicals, *Proc. Natl. Acad. Sci. U.S.A. 93*, 2448−2453.
20. Patel, R. P., Moellering, D., Murphy-Ullrich, J., Jo, H., Beckman, J. S., and Darley-Usmar, V. M. (2000) Cell signaling by reactive nitrogen and oxygen species in atherosclerosis, *Free Radical Biol. Med. 28*, 1780−1794.
21. Wink, D. A., Kasprzak, K. S., Maragos, C. M., Elespuru, R. K., Misra, M., Dunams, T. M., Cebula, T. A., Koch, W. H., Andrews, A. W., Allen, J. S., et al. (1991) DNA deaminating ability and genotoxicity of nitric oxide and its progenitors, *Science 254*, 1001−1003.
22. Nguyen, T., Brunson, D., Crespi, C. L., Penman, B. W., Wishnok, J. S., and Tannenbaum, S. R. (1992) DNA damage and mutation in human cells exposed to nitric oxide in vitro, *Proc. Natl. Acad. Sci. U.S.A. 89*, 3030−3034.
23. Caulfield, J. L., Wishnok, J. S., and Tannenbaum, S. R. (1998) Nitric oxide-induced deamination of cytosine and guanine in deoxynucleosides and oligonucleotides, *J. Biol. Chem. 273*, 12689−12695.
24. Yermilov, V., Rubio, J., Becchi, M., Friesen, M. D., Pignatelli, B., and Ohshima, H. (1995) Formation of 8-nitroguanine by the reaction of guanine with peroxynitrite in vitro, *Carcinogenesis 16*, 2045−2050.
25. Yermilov, V., Rubio, J., and Ohshima, H. (1995) Formation of 8-nitroguanine in DNA treated with peroxynitrite in vitro and its rapid removal from DNA by depurination, *FEBS Lett. 376*, 207−210.
26. Lewis, R. S., Tannenbaum, S. R., and Deen, W. M. (1995) Kinetcs of *N*-nitrosatino in oxygenated nitric oxide solutions at physiological pH: role of nitrous anhydride and effects of phosphate and chloride, *J. Am. Chem. Soc. 117*, 3933−3939.
27. Burney, S., Caulfield, J. L., Niles, J. C., Wishnok, J. S., and Tannenbaum, S. R. (1999) The chemistry of DNA damage from nitric oxide and peroxynitrite, *Mutat. Res. 424*, 37−49.
28. deRojas-Walker, T., Tamir, S., Ji, H., Wishnok, J. S., and Tannenbaum, S. R. (1995) Nitric oxide induces oxidative damage in addition to deamination in macrophage DNA, *Chem. Res. Toxicol. 8*, 473−477.
29. Shafirovich, V., Mock, S., Kolbanovskiy, A., and Geacintov, N. E. (2002) Photochemically catalyzed generation of site-specific 8-nitroguanine adducts in DNA by the reaction of long-lived neutral guanine radicals with nitrogen dioxide, *Chem. Res. Toxicol. 15*, 591−597.
30. Joffe, A., Mock, S., Yun, B. H., Kolbanovskiy, A., Geacintov, N. E., and Shafirovich, V. (2003) Oxidative generation of guanine radicals by carbonate radicals and their reactions with nitrogen dioxide to form site specific 5-guanidino-4-nitroimidazole lesions in oligodeoxynucleotides, *Chem. Res. Toxicol. 16*, 966−973.
31. Hsieh, Y. S., Chen, B. C., Shiow, S. J., Wang, H. C., Hsu, J. D., and Wang, C. J. (2002) Formation of 8-nitroguanine in tobacco cigarette smokers and in tobacco smoke-exposed Wistar rats, *Chem. Biol. Interact. 140*, 67−80.
32. Ma, N., Adachi, Y., Hiraku, Y., Horiki, N., Horiike, S., Imoto, I., Pinlaor, S., Murata, M., Semba, R., and Kawanishi, S. (2004) Accumulation of 8-nitroguanine in human gastric epithelium induced by *Helicobacter pylori* infection, *Biochem. Biophys. Res. Commun. 319*, 506−510.
33. Pinlaor, S., Hiraku, Y., Ma, N., Yongvanit, P., Semba, R., Oikawa, S., Murata, M., Sripa, B., Sithithaworn, P., and Kawanishi, S. (2004) Mechanism of NO-mediated oxidative and nitrative DNA damage in hamsters infected with Opisthorchis viverrini: a model of inflammation-mediated carcinogenesis, *Nitric* Oxide *11*, 175−183.
34. Ding, X., Hiraku, Y., Ma, N., Kato, T., Saito, K., Nagahama, M., Semba, R., Kuribayashi, K., and Kawanishi, S. (2005) Inducible nitric oxide synthase-dependent DNA damage in mouse model of inflammatory bowel disease, *Cancer Sci. 96*, 157−163.
35. Loeb, L. A., and Preston, B. D. (1986) Mutagenesis by apurinic/apyrimidinic sites, *Annu. Rev. Genet. 20*, 201−230.
36. Shibutani, S., Takeshita, M., and Grollman, A. P. (1997) Translesional synthesis on DNA templates containing a single abasic site: a mechanistic study of the A rule, *J. Biol. Chem. 272*, 13916−13922.
37. Hubscher, U., Maga, G., and Spadari, S. (2002) Eukaryotic DNA polymerases, *Annu. Rev. Biochem. 71*, 133−163.
38. Masutani, C., Araki, M., Yamada, A., Kusumoto, R., Nogimori, T., Maekawa, T., Iwai, S., and Hanaoka, F. (1999) Xeroderma pigmentosum variant (XP-V) correcting protein from HeLa cells has a thymine dimer bypass DNA polymerase activity, *EMBO J. 18*, 3491−3501.
39. Ogi, T., Kato, T., Jr., Kato, T., and Ohmori, H. (1999) Mutation enhancement by DINB1, a mammalian homologue of the *Escherichia coli* mutagenesis protein dinB, *Genes Cells 4*, 607−618.
40. Gerlach, V. L., Aravind, L., Gotway, G., Schultz, R. A., Koonin, E. V., and Friedberg, E. C. (1999) Human and mouse homologs of *Escherichia coli* DinB (DNA polymerase IV), members of the UmuC/DinB superfamily, *Proc. Natl. Acad. Sci. U.S.A. 96*, 11922−11927.
41. Goodman, M. F., and Tippin, B. (2000) The expanding polymerase universe, *Nat. Rev. Mol. Cell Biol. 1*, 101−109.
42. Kunkel, T. A., Pavlov, Y. L., and Bebenek, K. (2003) Functions of human DNA polymerases η, κ and ι suggested by their properties, including fidelity with undamaged DNA templates, *DNA Repair 3*, 135−149.
43. Shibutani, S. (1993) Quantitation of base substitutions and deletions induced by chemical mutagens during DNA synthesis in vitro, *Chem. Res. Toxicol. 6*, 625−629.
44. Shibutani, S., Suzuki, N., Matsumoto, Y., and Grollman, A. P. (1996) Miscoding properties of 3,N^4-etheno-2′-deoxycytidine in reactions catalyzed by mammalian DNA polymerases, *Biochemistry 35*, 14992−14998.
45. Mendelman, L. V., Boosalis, M. S., Petruska, J., and Goodman, M. F. (1989) Nearest neighbor influences on DNA polymerase insertion fidelity, *J. Biol. Chem. 264*, 14415−14423.
46. Mendelman, L. V., Petruska, J., and Goodman, M. F. (1990) Base mispair extension kinetics. Comparison of DNA polymerase alpha and reverse transcriptase, *J. Biol. Chem. 265*, 2338−2346.

47. Suzuki, T., Matsumura, Y., Ide, H., Kanaori, K., Tajima, K., and Makino, K. (1997) Deglycosylation susceptibility and base-pairing stability of 2′-deoxyoxanosine in oligodeoxynucleotide, *Biochemistry 36*, 8013−8019.
48. Maniatis, T., Fritsch, E. F., and Sambrook, J. (1982) *Molecular Cloning: A Laboratory Manual*, Cold Spring Harbor Laboratory Press, Cold Spring Harbor, NY.
49. Clark, J. M., Joyce, C. M., and Beardsley, G. P. (1987) Novel blunt-end addition reactions catalyzed by DNA polymerase I of *Escherichia coli*, *J. Mol. Biol. 198*, 123−127.
50. Terashima, I., Suzuki, N., Dasaradhi, L., Tan, C.-K., Downey, K. M., and Shibutani, S. (1998) Translesional synthesis on DNA templates containing an estrogen quinone derived adduct: N^2-(2-hydroxyestron-6-yl)-2′-deoxyguanosine and N^6-(2-hydroxyestron-6-yl)-2′-deoxyadenosine, *Biochemistry 37*, 13807−13815.
51. Yasui, M., Suzuki, N., Miller, H., Matsuda, T., Matsui, S., and Shibutani, S. (2004) Translesion synthesis past 2′-deoxyxanthosine, a nitric oxide-derived DNA adduct, by mammalian DNA polymerases, *J. Mol. Biol. 344*, 665−674.
52. Roy, K. B., and Miles, H. T. (1983) Tautomerism and ionization of xanthosine, *Nucleosides Nucleotides 2*, 231−242.
53. Rogstad, K. N., Jang, Y. H., Sowers, L. C., and Goddard, W. A. (2003) First principles calculations of the pK_a values and tautomers of isoguanine and xanthine, *Chem. Res. Toxicol. 16*, 1455−1462.
54. Eritja, R., Horowitz, D. M., Walker, P. A., Ziehler-Martin, J. P., Boosalis, M. S., Goodman, M. F., Itakura, K., and Kaplan, B. E. (1986) Synthesis and properties of oligonucleotides containing 2′-deoxynebularine and 2′-deoxyxanthosine, *Nucleic Acids Res. 14*, 8135−8153.
55. Vongchampa, V., Dong, M., Gingipalli, L., and Dedon, P. (2003) Stability of 2′-deoxyxanthosine in DNA, *Nucleic Acids Res. 31*, 1045−1051.
56. Brown, T., and Hunter, W. N. (1997) Non-Watson-Crick base associations in DNA and RNA revealed by single-crystal X-ray diffraction methods: mismatches, modified bases, and nonduplex DNA, *Biopolymers 44*, 91−103.
57. Prive, G. G., Heinemann, U., Chandrasegaran, S., Kan, L. S., Kopka, M. L., and Dickerson, R. E. (1987) Helix geometry, hydration, and G:A mismatch in a B-DNA decamer, *Science 238*, 498−504.
58. Juedes, M. J., and Wogan, G. N. (1996) Peroxynitrite-induced mutation spectra of pSP189 following replication in bacteria and in human cells, *Mutat. Res. 349*, 51−61.
59. Pamir, B., and Wogan, G. N. (2003) Carbon dioxide modulation of peroxynitrite-induced mutagenesis of the supF gene in pSP189, *Chem. Res. Toxicol. 16*, 487−492.
60. Shibutani, S., Takeshita, M., and Grollman, A. P. (1991) Insertion of specific bases during DNA synthesis past the oxidation-damaged base 8-oxodG, *Nature 349*, 431−434.
61. Haracska, L., Yu, S.-L., Johnson, R. E., Prakash, L., and Prakash, S. (2000) Efficient and accurate replication in the presence of 7,8-dihydro-8-oxoguanine by DNA polymerase η, *Nat. Genet. 25*, 458−461.

BI050276P